Bone 49 (2011) 1232–1241

Contents lists available at SciVerse ScienceDirect

Bone

journal homepage: www.elsevier.com/locate/bone

Original Full Length Article

Lathyrism-induced alterations in collagen cross-links influence the mechanical properties of bone material without affecting the mineral

E.P. Paschalis [a,*], D.N. Tatakis [b,c], S. Robins [d], P. Fratzl [e], I. Manjubala [e], R. Zoehrer [a,1], S. Gamsjaeger [a], B. Buchinger [a], A. Roschger [a], R. Phipps [f], A.L. Boskey [g], E. Dall'Ara [h], P. Varga [h], P. Zysset [h], K. Klaushofer [a], P. Roschger [a]

[a] Ludwig Boltzmann Institute of Osteology at the Hanusch Hospital of WGKK and AUVA Trauma Centre Meidling, 1st Medical Department, Hanusch Hospital, Heinrich Collin Str. 30, A-1140 Vienna, Austria
[b] Division of Periodontology, The Ohio State University, Columbus, OH, USA
[c] Visiting Professor, King Saud University, Riyadh, Saudi Arabia
[d] Matrix Biochemistry, Rowett Institute of Nutrition and Health, University of Aberdeen, Aberdeen, Scotland, UK
[e] Max Planck Institute of Colloids and Interfaces, Department of Biomaterials, Research Campus Golm, Potsdam, Germany
[f] Dept. of Pharmacology, Husson University, ME, USA
[g] Hospital for Special Surgery, New York, NY, USA
[h] Institut für Leichtbau und Struktur-Biomechanik, TU Wien, Vienna, Austria

ARTICLE INFO

Article history:
Received 27 May 2011
Revised 24 August 2011
Accepted 26 August 2011
Available online 2 September 2011

Edited by: R. Baron

Keywords:
Collagen
Collagen cross-links
β-aminopropionitrile
Bone strength
Bone quality
Bone formation

ABSTRACT

In the present study a rat animal model of lathyrism was employed to decipher whether anatomically confined alterations in collagen cross-links are sufficient to influence the mechanical properties of whole bone. Animal experiments were performed under an ethics committee approved protocol. Sixty-four female (47 day old) rats of equivalent weights were divided into four groups (16 per group): Controls were fed a semi-synthetic diet containing 0.6% calcium and 0.6% phosphorus for 2 or 4 weeks and β-APN treated animals were fed additionally with β-aminopropionitrile (0.1% dry weight). At the end of this period the rats in the four groups were sacrificed, and L2–L6 vertebra were collected. Collagen cross-links were determined by both biochemical and spectroscopic (Fourier transform infrared imaging (FTIRI)) analyses. Mineral content and distribution (BMDD) were determined by quantitative backscattered electron imaging (qBEI), and mineral maturity/crystallinity by FTIRI techniques. Micro-CT was used to describe the architectural properties. Mechanical performance of whole bone as well as of bone matrix material was tested by vertebral compression tests and by nano-indentation, respectively.

The data of the present study indicate that β-APN treatment changed whole vertebra properties compared to non-treated rats, including collagen cross-links pattern, trabecular bone volume to tissue ratio and trabecular thickness, which were all decreased ($p<0.05$). Further, compression tests revealed a significant negative impact of β-APN treatment on maximal force to failure and energy to failure, while stiffness was not influenced. Bone mineral density distribution (BMDD) was not altered either. At the material level, β-APN treated rats exhibited increased Pyd/Divalent cross-link ratios in areas confined to a newly formed bone. Moreover, nano-indentation experiments showed that the E-modulus and hardness were reduced only in newly formed bone areas under the influence of β-APN, despite a similar mineral content.

In conclusion the results emphasize the pivotal role of collagen cross-links in the determination of bone quality and mechanical integrity. However, in this rat animal model of lathyrism, the coupled alterations of tissue structural properties make it difficult to weigh the contribution of the anatomically confined material changes to the overall mechanical performance of whole bone. Interestingly, the collagen cross-link ratio in bone forming areas had the same profile as seen in actively bone forming trabecular surfaces in human iliac crest biopsies of osteoporotic patients.

© 2011 Elsevier Inc. Open access under CC BY-NC-ND license.

* Corresponding author at: Ludwig Boltzmann Institute of Osteology, Hanusch Krankenhaus, Heinrich Collin Str. 30, A-1140 Vienna, Austria.
E-mail addresses: eleftherios.paschalis@osteologie.at (E.P. Paschalis), tatakis.1@osu.edu (D.N. Tatakis), s.robins@abdn.ac.uk (S. Robins), Peter.Fratzl@mpikg.mpg.de (P. Fratzl), i.manjubala@mpikg.mpg.de (I. Manjubala), Ruth.Zoehrer@flinders.edu.au (R. Zoehrer), sonja.gamsjaeger@osteologie.at (S. Gamsjaeger), birgit.buchinger@osteologie.at (B. Buchinger), andreas.roschger@osteologie.at (A. Roschger), PhippsR@husson.edu (R. Phipps), boskeya@hss.edu (A.L. Boskey), edallara@ilsb.tuwien.ac.at (E. Dall'Ara), vpeter@ilsb.tuwien.ac.at (P. Varga), philippe.zysset@ilsb.tuwien.ac.at (P. Zysset), klaus.klaushofer@osteologie.at (K. Klaushofer), paul.roschger@osteologie.at (P. Roschger).
[1] Current address: School of Chemical and Physical Sciences, Flinders University, GPO Box 2100, Adelaide, SA 5001, Australia.

8756-3282 © 2011 Elsevier Inc. Open access under CC BY-NC-ND license.
doi:10.1016/j.bone.2011.08.027

Introduction

Historically osteoporosis has been defined as a disease in which there is "too little bone, but what there is, is normal" [1]. Although there is extensive data indicating this definition has to be modified [2], to date, working definitions of osteoporosis are based predominantly on bone mass. While evaluations of bone mass are of great clinical importance, they do not provide any information about the quality of the remaining bone mineral and matrix (in particular collagen) components [2].

The intermolecular cross-linking of bone collagen is intimately related to the way collagen molecules are arranged in fibrils. Six major collagen cross-links have been established as naturally occurring intermolecular cross-links. They are (i) dehydrodihydroxylysinonorleucine (deH-DHLNL) which exists primarily in its ketoamine form, hydroxylysine-5-keto-norleucine (HLKNL), (ii) dehydrohydroxylysinonorleucine (deH-HLNL) which is also present as the ketoamine, lysine-5-keto-norleucine (LKNL), (iii) pyridinoline (PYD), (iv) deoxypyridinoline (DPD; lysyl analog of PYD), (v) pyrroles (PYL and DPL), and (vi) histidinohydroxylysinonorleucine (HHL). The first two are reducible with borohydride (their reduced forms are referred to as DHLNL, and HLNL, respectively) and the rest are non-reducible compounds [3–6]. In mineralized tissue collagen the predominant cross-links are: HLKNL, LKNL, PYD, DPD, and pyrroles [7,8].

Data exist showing that the properties of collagen affect the mechanical strength of bone [9–11]. Recent clinical reports have correlated plasma homocysteine levels and bone fragility [12–15]. Homocysteine affects bone formation areas and in particular collagen cross-links [16]. The homocysteine-induced changes in collagen cross-links at trabecular bone forming and resorbing surfaces are similar to those seen in osteoporotic and fragility fracture patients [17,18]. Moreover, in a recent report employing spectroscopic analysis of iliac crest biopsies from 54 women (aged 30–83 yr; 32 with fractures, 22 without) who had significantly different spine but not hip Bone Mineral Density (BMD), it was found that cortical and cancellous bone collagen cross-link ratio strongly correlated positively with fracture incidence [19], further emphasizing the contribution of collagen cross-links in determining bone strength. In addition, in studies where there was a deviation between BMD values and bone strength, the spectroscopically determined pyridinoline (PYD)/divalent collagen cross-link ratio always correlated with bone strength [18–21]. One puzzling fact with these studies was the observation that the alterations in collagen cross-link ratio (PYD/divalent) were anatomically restricted to actively forming trabecular surfaces (based on either histologic stains or the presence of primary mineralized packets), while the rest of the bone seemed unaffected.

The purpose of the present study was to investigate whether anatomically confined alterations in collagen cross-links are sufficient to influence the mechanical performance of whole bone, employing the well-established β-aminopropionitrile (β-APN) treated rat model [22,23]. β-aminopropionitrile inhibits the lysyl oxidase-mediated formation of lysine aldehydes which are precursors of the major divalent and trivalent bone collagen cross-link moieties (HLKNL, LKNL, PYD, DPD). Vertebral bone was analyzed by μCT, micro finite element analysis (μFE), quantitative backscatter electron imaging (qBEI), compression mechanical testing, nanoindentation, and FTIRI analysis. Collagen cross-links were determined both chemically and spectroscopically.

Materials and methods

Animals

Under an Ohio State University IACUC-approved protocol, sixty-four female (47 day old) rats of equivalent weights were divided into four groups (16 per group): 2 control and 2 treatment groups. Controls were fed a semi-synthetic diet containing 0.6% calcium and 0.6% phosphorus as published elsewhere [24] for 2 or 4 weeks and β-APN treated animals were fed a diet inclusive of β-aminopropionitrile (0.1% dry weight) for 2 or 4 weeks . The 2 and 4 week-time points were used to allow formation of new bone with varying degrees of cross-linking in limited anatomical areas, without affecting the whole bone. Rats were sacrificed at the assigned time points and intact spines were harvested, dissected free from soft tissue and stored in 70% ethanol.

Chemical analysis of collagen cross-links

L3 vertebra from each animal were equilibrated with phosphate buffered saline, pH 7.8, pulverized and reduced with KBH_4 for 1 h. After this time, the pH was adjusted to 4 with acetic acid to destroy excess reagent, the tissue washed extensively with water and freeze dried. The reduced bone was hydrolyzed in 6 M HCl at 107 °C for 22 h and the acid was removed by evaporation. Following preliminary fractionation of cross-linked amino acids by partition chromatography, the intermediate compounds (DHLNL and HLNL) were assayed by ion-exchange chromatography with post-column derivatization and the mature bonds (PYD and DPD) were quantified using RP-HPLC using their natural fluorescence, as described previously [25]. Cross-link concentrations were expressed relative to collagen content determined by colorimetric measurement of hydroxyproline in the original hydrolysate. It should be noted here that both cortical and trabecular bone were included in the analysis.

μCT

The endplates of each L2 vertebra were carefully removed with a low speed diamond-coated saw (Isomet, Buehler, Germany) to provide samples with a height of approximately 3 mm. The vertebral body was then isolated from the posterior elements and one of the plane surfaces was glued on a carbon rod with a thin layer of cyanoacrylate glue. The other surface was polished to achieve parallel faces. The average final height was 2.5 mm. The vertebral body was scanned in 70% ethanol by μCT with a 12 μm voxel size (μCT40, Scanco, Switzerland). The reconstructions were segmented with an optimal threshold, separated into trabecular and cortical compartments and standard histomorphometric parameters were computed with the manufacturer's software (IPL, Scanco, Switzerland).

qBEI

Vertebrae (L5) were fixed in 70% ethanol, dehydrated through a graded series of ethanol and embedded undecalcified in polymethylmethacrylate (PMMA). About 5 millimeter thick blocks containing a sagittal vertebral bone section were cut using a low speed diamond saw (Buehler Isomed, Lake Pluff, USA). The section surface was ground with sand paper and subsequently polished by a diamond suspension (3 and 1 μm grain size, respectively) using a precision polishing device (MP5 Logitech, Ltd, Glasgow, Scotland). The sample surface was carbon coated prior to qBEI. A digital electron microscope (DSM 962, Zeiss, Oberkochen, Germany) equipped with a four quadrant semiconductor BE detector was used for backscattered electron imaging. The accelerating voltage of the electron beam was adjusted to 20 kV, the probe current to 110 pA, and the working distance to 15 mm. The digital backscattered (BE) images of trabecular bone areas were acquired by a single frame with a scan speed of 100 s/frame and a pixel resolution of 1 μm. Areas with high backscattered electron intensities – light gray levels – represent mineralized matrix with high Ca contents, whereas areas with low intensities – dark gray levels – indicate low mineral density. For the characterization and quantification of changes in the bone mineralization density distribution (BMDD) curve, four outcomes were used: CaMean (the weight mean calcium content of the bone area obtained from the integrated

area under the BMDD curve), CaPeak (the mode of calcium content indicated by the peak position in the BMDD diagram), CaWidth (the heterogeneity of mineralization caused by the coexistence of BSU of different ages measured at the full width at one-half maximum of the BMDD-peak), CaLow (reflects the fraction low mineralized bone areas (<17.68 wt Ca)). Details of the analysis method have been published previously [26].

Additionally, these qBEI images were also used later, to evaluate the mean gray level/mineral content (Ca_{Ind}) at the nanoindentation sites similar as described in Ref. [27].

Mechanical testing

After μCT scanning, the L2 vertebral bodies were rehydrated, mounted in a servo-hydraulic testing system (858 Mini Bionix II, MTS, USA), preconditioned with 10 cycles in the elastic range and tested to failure in axial compression with a rate of 0.033 mm/s. Stiffness, maximal load to failure, and energy to failure were computed from the resulting force–displacement curves. A mean tissue modulus for each vertebral body was then back-calculated from the experimental stiffness using a 12 μm resolution, homogeneous, linear elastic ($v = 0.3$) finite element model of the same loading scenario.

Nanoindentation was performed using a Scanning Nanoindenter (Hysitron Inc., Minneapolis, USA) with a Berkovich diamond indenter tip as described elsewhere [28]. The calibration of the instrument was performed by doing indents of increasing depth in fused quartz with a known reduced modulus of 72 GPa. The material properties of the diamond tip are known such as the Poisson's ratio is 0.07 and elastic modulus of the tip is 1140 GPa. Automated area scans of indents were performed using moving sample stage, which has a positional resolution of 1 μm. There was a distance of 10 to 11 μm between indents. A thermal drift correction factor was introduced automatically before each indent, by measuring the drift for 20 s. Before every indent, there was a relaxation time of 60 s and 45 s for stabilizing digital feedback loop. More than 100 indents were made in the selected region of size varying from 300 to 500 μm. A maximum load of 5000 μN was used. Anatomical areas were selected based on qBEI images, and results were normalized for calcium content. The elastic modulus was calculated using the method of Oliver and Pharr [29], by fitting the unloading curve with a second order polynomial, differentiating and therefore evaluating the elastic recovery at maximum load to determine the contact depth. The parameters measured during the experiment were peak load (Pmax), peak displacement hmax, contact area Ac, and stiffness S. The stiffness was calculated from the slope of the initial unloading curve; the region between 20 and 95% of the maximum load was used to determine the slope of the unloading curve. The hardness H and reduced modulus Er are calculated from unloading contact stiffness, S, and the indenter contact area Ac:

$$H = P_{max}/A_c$$

$$Er = \pi^{1/2} S/2{A_c}^{1/2}$$

FTIRI analyses

Thin sections (~4 μm) were cut from the L5 vertebrae, and spectral images acquired in the area of trabecular bone using a Bruker Equinox 55 (Bruker Optics) spectrometer interfaced to a Mercury Cadmium Telluride (MCT) focal plane array detector (64×64 array) imaged onto the focal plane of an IR microscope (Bruker Hyperion 3000; Bruker Optics). Each area imaged was 400×400 μm, corresponding to an optimal spatial resolution of ~6.3×6.3 μm. Spectral resolution was 4 cm^{-1}. Background spectral images were collected under identical conditions from the same BaF_2 windows at the beginning and end of each experiment to ensure instrument stability. Both instruments were continuously powered to minimize warm-up instabilities and purged with dry-air (Bruker Optics) to minimize the water vapor and CO_2 interference. Following this, individual spectra were extracted from trabecular surfaces that were exhibiting either primary mineralization packets, or resorption pits, based on the previously acquired qBEI images (six different trabecular surfaces per animal were analyzed).

The individual spectra were processed as published elsewhere to derive the following spectroscopic parameters: (i) Mineral/matrix ratio (integrated areas under the phosphate (mineral) 900–1200 cm^{-1} and amide I 1592–1728 cm^{-1} (matrix; mainly collagen) absorbance peaks, respectively; corresponds to ash weight measurements) [30], (ii) mineral maturity/crystallinity (through curve-fitting of the phosphate (mineral) 900–1200 cm^{-1} peak and the calculation of the 1030 to 1020 cm^{-1} sub-band peak area) [31,32], and (iii) the ratio of PYD/divalent collagen cross-links (through curve-fitting of the Amide I and II peaks and the calculation of the 1660 to 1690 cm^{-1} sub-band peak area) [33]. For each animal, the values of each parameter at a particular anatomical site (forming or resorbing) were averaged and the resultant value was treated as a single statistical unit.

Statistical analyses

For each parameter, mean and standard deviation for the two groups at the two time points were reported. Two-way ANOVA with Bonferroni post-test analysis was applied to address the following three questions: i) does age have the same effect at all values of treatment (interaction), ii) does age affect the result, and iii) does treatment affect the result. Where this type of analysis indicated significant differences, additional comparisons were made employing unpaired *t*-test. Additionally, 2-way correlations between spectroscopically determined pyd/divalent collagen cross-link ratio, structural and mechanical properties were explored using Spearman's test. Significance was assigned to $p < 0.05$.

Results

The animals did not show any effect of the diet during the treatment period. There was no statistical difference in weight between the control and β-APN-treated animal groups at either time point although both groups gained weight over the two week period (data not shown).

Two-way ANOVA of qBEI measurements also showed no statistically significant differences between the animal groups at either time point in any of the four outcomes monitored (Table 1), with the exception of CaPeak which was dependent on animal age but not treatment.

Table 1
BMDD parameters of cancellous bone in untreated rats (control) compared with β-APN treated rats after 2 and 4 weeks of treatment.

	2 weeks		4 weeks		Two way ANOVA (p values)		
BMDD parameters	Control	β-APN	Control	β-APN	Inter-action	Treatment	Age
CaMean (wt.% Ca)	22.62 (0.78)	23.00 (0.65)	23.07 (0.57)	23.66 (0.75)	*ns*	*ns*	*ns*
CaPeak (wt.% Ca)	22.88 (0.68)	23.01 (0.64)	23.26 (0.65)	24.00 (0.60)	*ns*	*ns*	*
CaWidth (Δwt.% Ca)	3.88 (0.40)	3.71 (0.31)	3.54 (0.09)	3.87 (0.24)	*ns*	*ns*	*ns*
CaLow (% B.Ar)	4.76 (1.08)	4.10 (0.71)	3.68 (0.70)	4.05 (0.96)	*ns*	*ns*	*ns*

BMDD parameter values are mean and (SD).
* $p < 0.05$.

Table 2
Summary of 2-way ANOVA analysis of the biochemically determined collagen cross-links as well as the spectroscopically determined collagen cross-link ratio (pyd/deH-DHLNL), along with the appropriate p-values. Statistical significance is noted by bold text.

	Interaction	Age	Treatment
DHLNL (biochemical)	*0.324*	**0.014**	**0.002**
HLNL	*0.373*	*0.616*	*0.104*
PYD	*0.093*	*0.755*	**0.026**
DPD	*0.759*	*0.232*	<**0.0001**
PYD/DPD	*0.250*	*0.433*	*0.080*
Biochemically determined PYD/divalent	**0.028**	**0.005**	**0.010**
Spectroscopically determined PYD/divalent at forming trabeculae	*0.514*	*0.616*	**0.001**
Spectroscopically determined PYD/divalent at periosteal surfaces	*0.609*	*0.790*	**0.0001**

Table 3
Summary of 2-way ANOVA analysis of the vertebral bone structural properties as determined by μCT, along with the appropriate p-values. Statistical significance is noted by bold text.

	Interaction	Age	Treatment
Trab_BV/TV	*0.443*	*0.454*	**0.0005**
Trab_TRI-SMI	*0.573*	*0.154*	**0.0002**
Trab_DT-Tb.Th	*0.482*	**0.012**	<**0.0001**
Trab_DIM-Z	*0.466*	**0.003**	*0.234*
Cort_DT-Ct.Th	*0.472*	<**0.0001**	<**0.0001**

Biochemical analysis indicated that changes in DHLNL were dependent on both animal age and treatment, while PYD and DPD were dependent only on treatment. The calculated PYD/divalent cross-link ratio was dependent on both animal age and treatment (Table 2). Further comparisons using unpaired t-tests showed significant differences in DHLNL, between control and β-APN-treated animals at the 4 week time point, and a time-dependent difference in the β-APN treated animals at 2 and 4 weeks (Fig. 1a). The concentration of the trivalent cross-link PYD was significantly different between the control and β-APN treated animals at the 4-week time point (Fig. 1b). The other trivalent collagen cross-link, DPD, was significantly different between control and treated animals at both time points (Fig. 1c). The calculated ratio between PYD/DHLNL was increased in both groups as a function of time, and was elevated in the 4 week treated animal group compared to the 2 week treated and the 4 week control groups (Fig. 1d).

Two-way ANOVA analysis (Table 3) of structural parameters determined by μ-CT analysis of vertebral bone revealed no interaction between factor age and treatment. Trabecular BV/TV and TRI-SMI were influenced only by treatment, trabecular thickness by age and treatment, and trabecular DIM-Z by age only. Additionally, cortical thickness was influenced by both age and treatment. Further statistical analysis employing unpaired t-tests a significantly lower BV/TV in the treated animals at 4 weeks compared to the corresponding controls (Fig. 2a). Differences in Structural Model Index (TRI-SMI) were also observed with age and in treated animals for 4 weeks compared to corresponding controls (Fig. 2b). Trabecular thickness was lower in the treated animals compared to their respective controls at both time points (Fig. 2c).

Analysis of the compression testing of vertebrae based on two-way ANOVA (Table 4) showed no significant interaction between factor age and treatment. Stiffness and maximum force to failure were affected by both age and treatment, energy to failure was affected only by treatment. The predicted tissue modulus (based on finite element analysis) was dependent on age but not treatment. Unpaired *t*-test comparisons showed significant increases in stiffness within each group as a function of time (age) (Fig. 3a). Significant increases

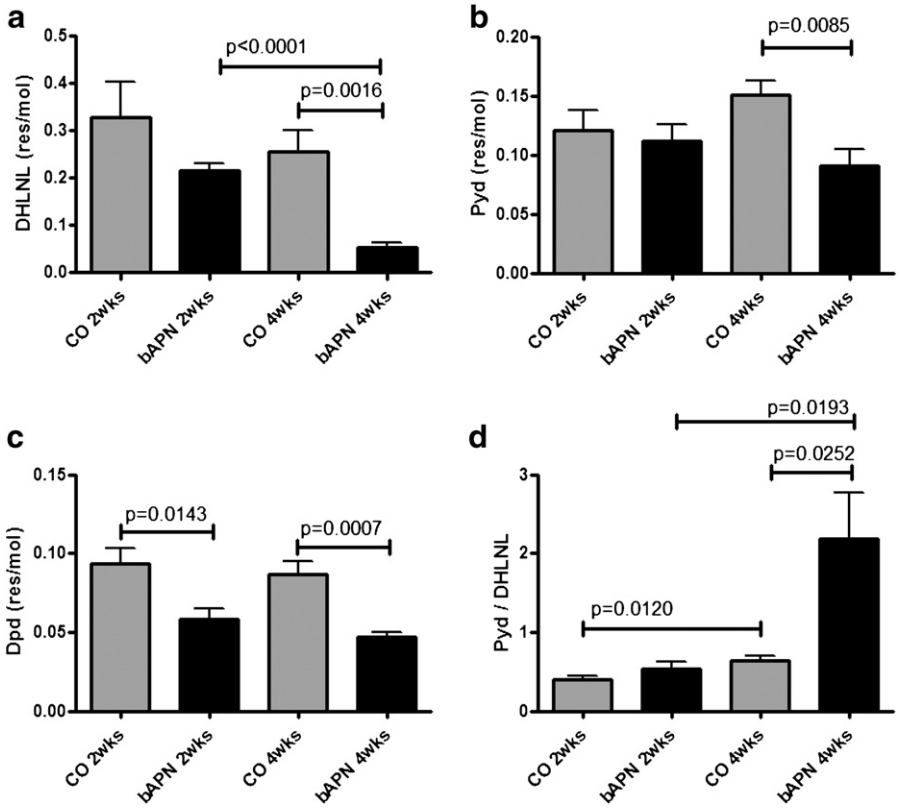

Fig. 1. Biochemical analysis of vertebrae revealed significant differences in DHLNL (a), PYD (b), and DPD (c) collagen cross-links between normal (CO) and treated (bAPN) animals. The ratio of PYD/DHLNL collagen cross-links exhibited the most dramatic differences (d). Significant differences among groups are shown by solid lines, and appropriate p values listed.

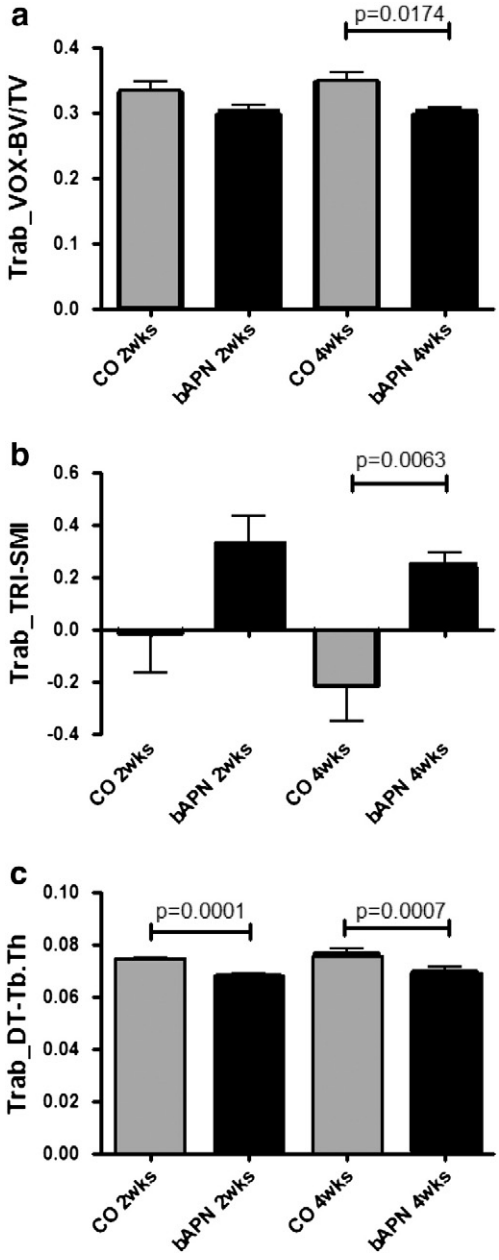

Fig. 2. μ-CT analysis of vertebral trabecular bone revealed a significantly lower BV/TV in the treated (bAPN) animals at 4 weeks compared to controls (CO) (a). Significant differences in structural model index (TRI-SMI) were also observed with age and in treated animals for 4 weeks compared to controls (b). Trabecular thickness was lower in the treated animals compared to their respective controls at both time points (c). Significant differences among groups are shown by solid lines, and appropriate p values listed.

in maximum force to failure were observed both as a function of age within each group, as well as in treated groups at both time points (Fig. 3b). Energy to failure was significantly lower in the treated for 4 weeks animals compared to respective controls (Fig. 3c). Interestingly, FE analysis based on the μ-CT data predicted significant differences only for the tissue modulus in the treated animal groups as a function of age (Fig. 3d).

The qBEI image taken before the nanoindentation experiment showed the typical region selected for testing in one β-APN treated rat (Fig. 4a) and the image observed by environmental scanning electron microscopy (ESEM) after indentation shows the line of indents marked by red circles (Fig. 4b). The ESEM image was overlaid on to the qBEI image and small square grids were placed over the indents and the quantitative mineral content at these points was extracted from the relevant pixels on the qBEI image taken before indentation (Fig. 4c). The mapping of calcium content from the qBEI measurements and the mapping of mechanical properties such as the indentation modulus, Er, and the hardness are shown in Figs. 4 (d–f). The calcium content was found to be lower in newly formed region near the outer sides of the trabeculae and, accordingly, lower stiffness and hardness values were observed in these newly formed bone regions. The relation between the indentation moduli and the local calcium content is represented in Fig. 4g. The values of the indentation modulus and of the hardness in the newly formed bone of the β-APN treated tissues are decreased by 35% ($p<0.001$) and 40% ($p<0.003$), respectively, compared to control samples in areas with 19 wt.% calcium or less, which typically correspond to newly formed bone. For older mature bone, with calcium content typically higher than 19 wt.%, there were no significant changes in the indentation modulus or in the hardness (Figs. 4h and i).

Spectroscopic analysis of L5 vertebrae revealed no significant differences between control and treated animals in mineral to matrix ratio as a function of either animal age or treatment (based on two-way ANOVA analysis; data not shown) in any of the surfaces analyzed. Additionally, there were no significant differences in mineral maturity/crystallinity at any of the examined surfaces between normal and treated groups at either time point (data not shown). On the other hand, two-way ANOVA analysis indicated that changes in the spectroscopically determined PYD/divalent collagen cross-link ratio were dependent on treatment but not age (Table 2), in the areas of periosteal (cortical) and primary mineralized trabecular surfaces. No differences were discernible in secondary mineralized trabecular surfaces (Fig. 5). Statistical comparisons based on unpaired t-tests indicated that there were significant differences in this ratio in primary mineralized trabecular areas (Fig. 6a), with treated animals exhibiting a significantly higher PYD/divalent collagen cross-link ratio compared to the corresponding controls, regardless of treatment duration. Since this is a ratio, the observed increase could be due to several possibilities regarding the change in the individual factors. To further discern the reason for the observed increase in the treated animals, the relative % area of the individual underlying bands (1660 and 1690 cm^{-1}, representative of Pyd and divalent collagen cross-links, respectively) were plotted (Fig. 6b), revealing a disproportionate decrease in Pyd and divalent collagen cross-links, in agreement with the biochemical analysis data. Similar findings were observed when the cortical periosteal surfaces were compared (Figs. 6c and d, respectively).

The results thus far indicated that β-APN treatment affected bone structural properties, collagen cross-links in anatomically confined areas (primary mineralized packets in trabecular, and periosteal cortical surfaces), and mechanical properties. The statistically significant correlations between these outcomes along with the Spearman's rho value are listed in Table 5. Stiffness correlates well with biochemically, and spectroscopically determined trabecular Pyd/divalent collagen cross-links, and cortical thickness (Ct.Th). Maximum force to failure correlates well with biochemically, and spectroscopically determined trabecular pyd/divalent collagen cross-links, TriSmi, Tb.Th, and Ct.Th. Finally, maximum energy to failure correlates well with biochemically determined Pyd/divalent collagen cross-link ratio, Ct.Th, and periosteal Pyd/divalent collagen cross-link ratio.

Table 4
Summary of 2-way ANOVA analysis of the vertebral bone actual mechanical properties (compression), as well as the predicted ones (through finite element analysis), along with appropriate p-values. Statistical significance is noted by bold text.

	Interaction	Age	Treatment
Stiffness	*0.709*	<**0.0001**	**0.022**
Maximum force to failure	*0.123*	<**0.0001**	<**0.0001**
Energy to failure	*0.389*	*0.097*	**0.014**
FE_stiffness	*0.402*	*0.268*	*0.201*
FE_tissue modulus	*0.537*	<**0.0001**	*0.473*

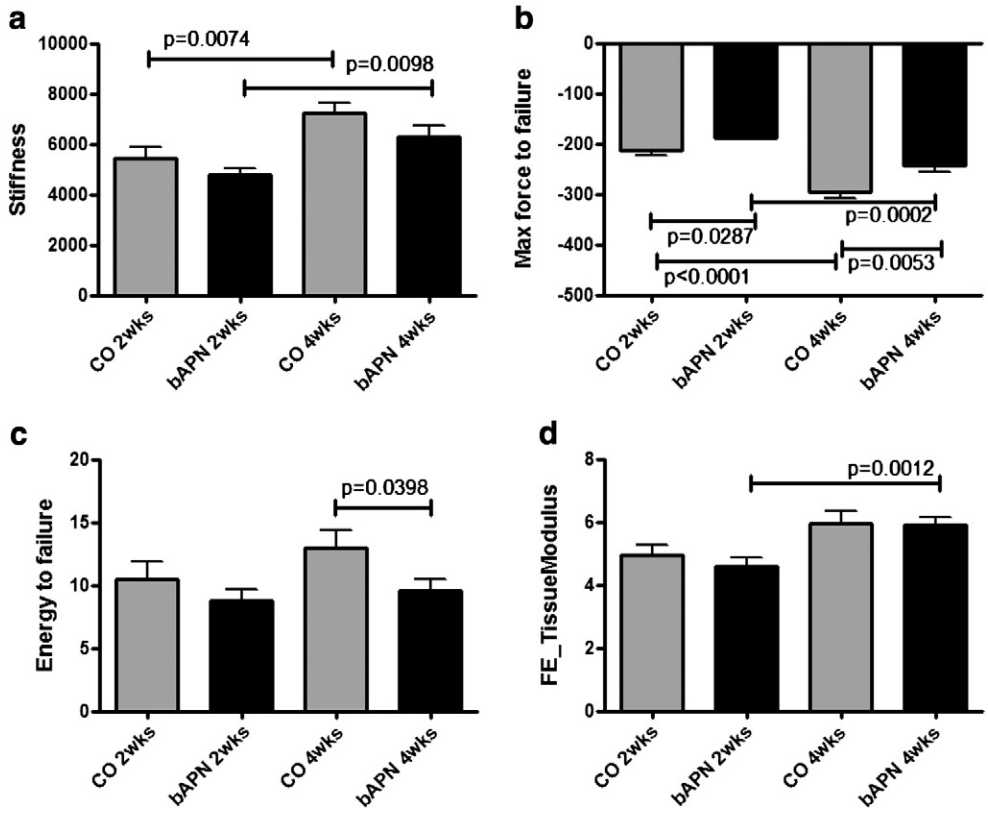

Fig. 3. Compression mechanical testing of vertebrae revealed significant increases in stiffness within each group as a function of time (a), significant increases in maximum force to failure both as a function of age within each group, as well as in treated groups at both time points (b), significantly lower energy to failure in the treated for 4 weeks animals compared to respective controls (c). Finite Element analysis based on the μ-CT data predicted significant differences only for the tissue modulus in the treated (bAPN) animal groups as a function of age (d). Significant differences among groups are shown by solid lines, and appropriate p values listed.

Discussion

The results of the present study employing a lathyritic rat animal model indicate that collagen cross-links coupled with structural changes are a major contributor to bone strength, in line with previously published reports in animal models and human tissue [22,23,34–39]. They also indicate a correlation with bone structural properties, in agreement with previously published results [40]. They additionally indicate that even when these changes are anatomically restricted (in the present case only in primary mineralized bone), coupled with changes in bone structural properties, they are sufficient to influence the mechanical performance of whole bone, even in the absence of concomitant mineral quantitative and/or qualitative properties alterations. Moreover, finite element analysis is not capable of predicting the full breadth of such an effect on bone strength.

Recent publications have reported that bone plastic deformation properties are determined not only by mineral content, but also by the organic matrix and interactions between these two components [41], and that tissue mineral density is an incomplete surrogate for tissue elastic modulus [42]. Bone structural and material properties (including mineral density expressed as mineral/matrix, mineral maturity/crystallinity and collagen cross-links) are important contributors to bone strength [2]. Moreover, the organic matrix is proposed to play an important role in alleviating damage to mineral crystallites, and to matrix/mineral interfaces, behaving like a soft wrap around mineral crystallites thus protecting them from the peak stresses, and homogenizing stresses within the bone composite [2,43,44]. The importance of collagen properties in determining bone strength is emphasized by several publications in the literature reporting altered collagen properties associated with fragile bone, in both animals and humans [6,17,18,22,34,37–39,45–51].

Employing FTIRI analyses, we have previously reported altered collagen cross-link ratio (PYD/divalent) in forming trabecular surfaces in osteoporotic patients and patients with fragility fractures [17,18]. The surprising finding was that these alterations compared to normal bone were restricted in forming surfaces only, thus whether these alterations were important contributors to bone fragility remained in question. To address this, an animal model was utilized in the present study to test the hypothesis that even anatomically confined alterations in collagen cross-links can affect whole bone mechanical performance independent of mineral. It has been previously shown that in vivo β-APN treatment causes significant changes in the mechanical properties of rat femora (26% decrease in failure stress and a 30% decrease in elastic modulus as determined in a bending test after 30 days of treatment) [22], and that it affects the cross-linking of collagen in the dosage used in the present study [52–56].

β-APN treatment, as expected, caused significant reductions in vertebral DHLNL, PYD, and DPD cross-links, as well as the calculated Pyd/divalent collagen cross-link ratio, as determined through biochemical analysis of whole bone homogenate. Interestingly, the alterations in divalent and trivalent cross-link concentrations were disproportionate; thus there were significant increases in the PYD/DHLNL ratio in the treated animals compared to corresponding controls whereas the treatment effects on HLNL were much less marked than for DHLNL. Although a relative decrease in the proportion of DHLNL with animal age may have contributed to the results, the observed changes were primarily due to the administration of β-APN. This inhibitor of lysyl oxidase might be expected to act equally on the divalent precursors of the non-reducible cross-links but their

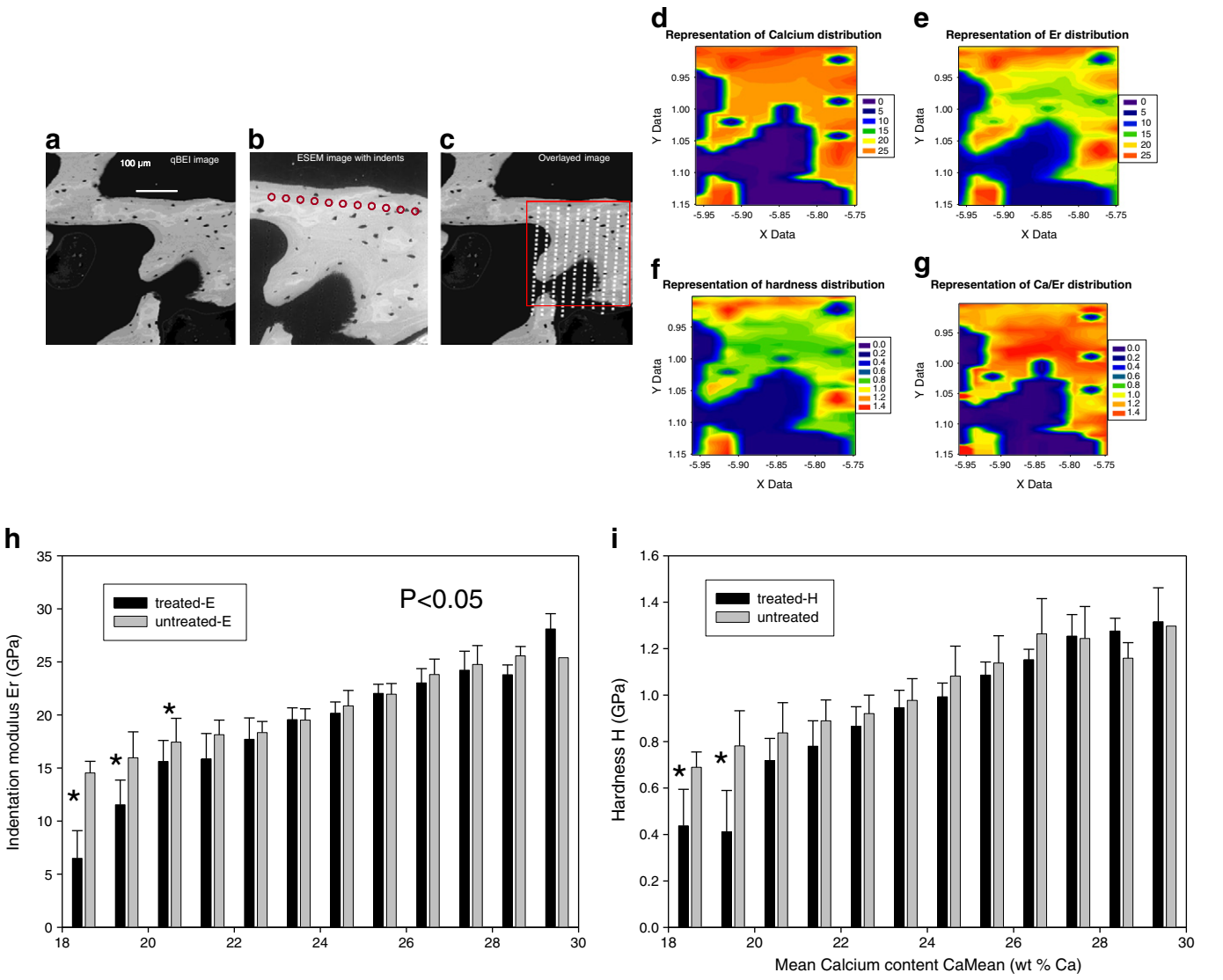

Fig. 4. The qBEI image taken before the nanoindentation experiment shows the typical region selected for testing in one β-APN treated rat (a) and the image observed by environmental scanning electron microscopy (ESEM) after indentation shows the line of indents marked by red circles (b). The ESEM image was overlaid on to the qBEI one, small square grids were placed over the indents and the quantitative mineral content at these points was extracted from the relevant pixels on the qBEI image taken before indentation (c). The mapping of calcium content from the qBEI measurements and the mapping of mechanical properties such as the indentation modulus, Er, and the hardness are shown in panels d–g. The elastic modulus and hardness are reduced in the treated samples (h and i), in the low calcium range (18–24 wt.%) of new bone, compared to untreated control samples.

relative concentrations is also affected by lysyl hydroxylase enzymes, LH1 and LH2b, which control hydroxylation of lysine in the helix and telopeptides, respectively. It is tempting to speculate that β-APN treatment may also affect other enzyme activities leading to disproportionate changes in amounts of cross-links.

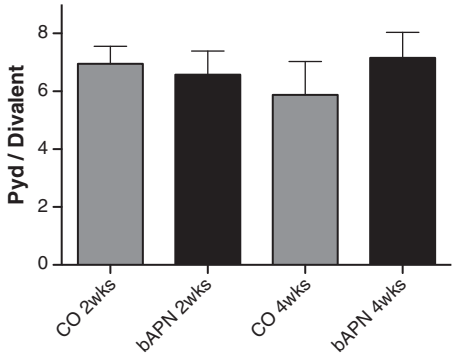

Fig. 5. No significant differences were observed among the 4 animal groups in the spectroscopically derived Pyd/divalent collagen cross-link ratio, when trabecular surfaces with evident resorption pits were considered.

FTIRI spectroscopic analysis of L5 vertebrae indicated that the alterations in the PYD/divalent ratio were confined in areas of trabecular surfaces with primary mineralization evident (i.e. forming), and periosteal surfaces of cortical bone, with β-APN-treated animals exhibiting a higher ratio compared to the corresponding controls. This increase was due to a disproportionate decrease of individual components, in excellent agreement with the results of the biochemical analysis. It should be emphasized that this increase does not imply that it is solely responsible for the observed differences in mechanical performance (decreases in all of collagen cross-links contribute to the inferior mechanical behavior of the treated animals), but Pyd, divalent, and the corresponding ratio are the only cross-links that can be spectroscopically monitored, to date. The discrepancy in the magnitude of change between the biochemically- and spectroscopically-determined ratio is most likely due to the fact that as we have previously reported the relationship between biologically- and spectroscopically-determined cross-link concentrations of Pyd is not a linear one [33]. Interestingly, while the biochemically determined PYD/divalent ratio alterations were dependent

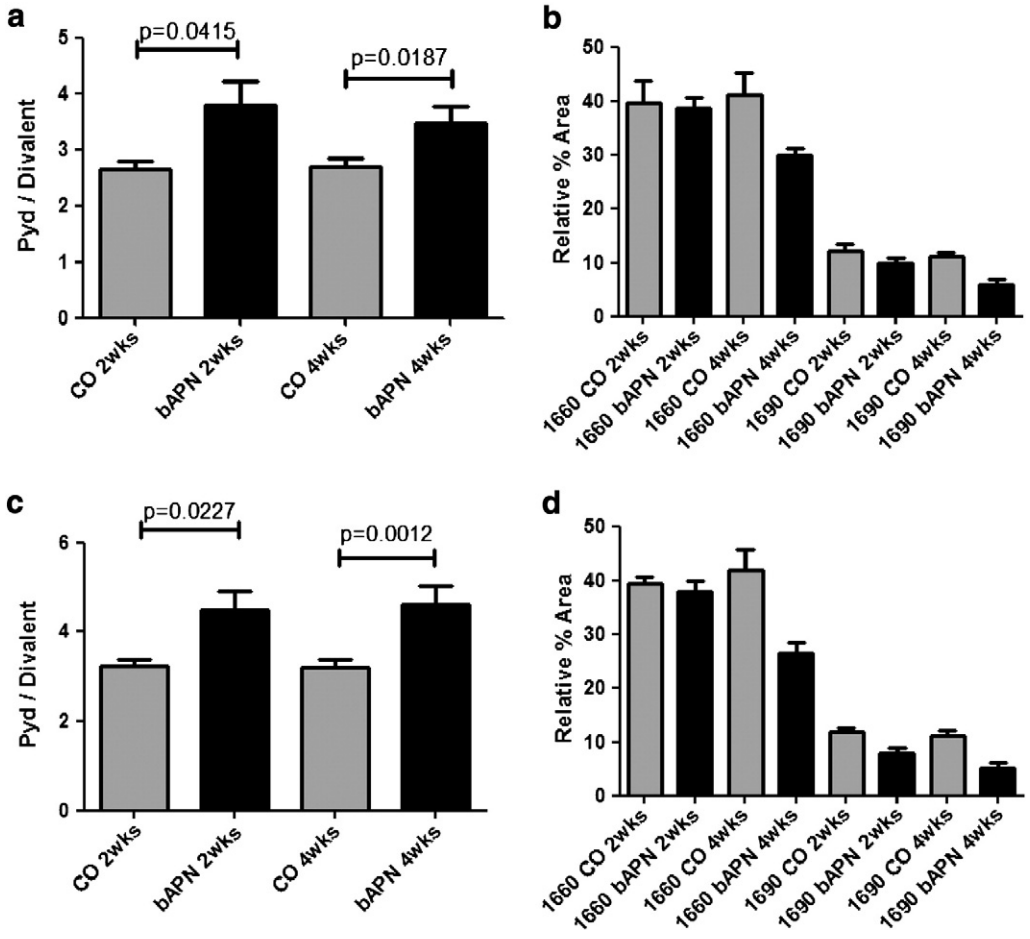

Fig. 6. Spectroscopic analysis of L5 vertebrae revealed significant differences in Pyd/divalent collagen cross-link ratio between normal (CO) and treated (bAPN) animals in primary mineralized areas of trabecular bone at both time points (a). When the individual components of this ratio are considered individually it becomes apparent that the source of the observed increase of the ratio is due to a disproportionate decrease of its individual components (b). Similar results were observed when cortical periosteal surfaces were considered (c and d). Significant differences among groups are shown by solid lines, and appropriate p values listed.

on both animal age and treatment, the spectroscopically determined ones were affected only by treatment (Table 2). This is most likely due to the fact that while the former is determined in bone of all tissue ages, the latter normalizes for tissue age through selection of anatomical areas of similar tissue age, and accentuates the importance of doing so when employing microscopic techniques for the determination of bone quality and in particular collagen properties, as differing tissue age is a confounding factor. When trabecular surfaces with evident resorption pits were considered, no significant differences were observed among the 4 animal groups. This is most likely attributable to the fact that this bone tissue is of older age, formed prior to β-APN administration, and thus was not affected by the lathyrogen administration.

Mineral content is a major contributor to bone stiffness. In the present study, mineral content was determined by two different methods: qBEI and FTIRI. The first technique provides the weight fraction mineral in each pixel/voxel of a scanned bone area by means of backscattered electron intensities (mirroring average atomic numbers) [26], while FTIRI provides information in a voxel of a thin bone section on amount of mineral normalized to the amount of organic matrix present by means of the ratio between the integrated areas of PO_4 (mineral) and amide I (mainly collagen) bands [57]. Both techniques have been shown to correspond to ash weight measurements [30,57,58], and be a good predictor of bone bending stiffness, correlating well with tissue stiffness and hardness [19,59–61]. In the present work, neither technique indicated any significant changes as a function of treatment.

Mineral maturity/crystallinity also contributes to bone strength [2,57]. In the present work, there were no differences between any

Table 5
Correlation coefficient (r) between bone mechanical and structural properties and spectroscopically determined pyd/divalent collagen cross-link ratio. Significant correlations are indicated by text in bold.

	Biochemically determined pyd/divalent collagen cross-link ratio (whole bone)	Spectroscopically determined pyd/divalent collagen cross-link ratio at primary mineralized trabecular surfaces	Spectroscopically determined pyd/divalent collagen cross-link ratio at periosteal cortical surfaces	BV/TV	TriSmi	Tb.Th	Ct.Th
Stiffness	**−0.564***	**−.856****	*ns*	*ns*	*ns*	*ns*	**.466****
Maximum force to failure	**0.540***	**.700****	*ns*	*ns*	**.313***	**−.316***	**−.658****
Maximum energy to failure	**−0.487****	*ns*	**−0.279***	*ns*	*ns*	*ns*	**.374****

* Correlation is significant at the 0.05 level (2-tailed).
** Correlation is significant at the 0.01 level (2-tailed).

of the animal groups investigated when equivalent anatomical locations were compared by FTIRI. This may be due to the fact that β-APN interferes with collagen post-translational modifications only, and the time of treatment (up to 4 weeks) was not sufficient for the changes in collagen post-translational modifications to induce significant changes in either mineral amount and/or quality.

Bone structural properties were also affected by β-APN treatment. While changes in trabecular BV/TV and TRI-SMI were affected by treatment only, changes in trabecular thickness and DIM-Z as well as cortical thickness were dependent on both animal age and treatment received, thus making it harder to interpret the latter in the context of altered collagen cross-links only (Table 3). These chemical and structural changes most likely contributed to the compromised mechanical properties in the treated animals. One potential reason for these observed changes in structural properties could be the fact that β-APN treatment affects osteoblasts both directly and indirectly [62,63], in addition to its well-established effect on collagen post-translational modifications. Unfortunately, the analyses reported in this manuscript cannot discern between the two effects.

Compression mechanical tests indicated differences among the various animal groups in bone stiffness, maximum force to failure, and energy to failure, the first two being affected by both animal age and treatment, while the third only by treatment. Cortical thickness correlated well with stiffness, maximum force to failure and maximum energy to failure. These data suggest a major role of cortical thickness in determining vertebral bone strength and in particular stiffness, a finding that is in agreement with previously published reports [64–69]. The biochemically determined Pyd/divalent collagen cross-links ratio correlated with stiffness (inversely), maximum force to failure, and maximum energy to failure (inversely). The fact that collagen cross-links correlate well with vertebral biomechanical properties is in agreement with previously published reports [36]. The spectroscopically determined PYD/divalent collagen cross-link ratio of primary mineralized trabecular bone correlated well with maximum force to failure and stiffness. Stiffness correlated negatively with the Pyd/divalent ratio (due to a disproportionate decrease in the individual components of the ratio). Additionally, this ratio at periosteal cortical surfaces correlated with maximum energy to failure (inversely).

Structural properties TriSmi and Tb.Th correlated only with maximum force to failure. In contrast, μFE analysis did not show any effect of treatment on stiffness, potentially due to the fact that the alteration of collagen cross-links was combined with preservation of the mineralization parameters as described by qBEI analysis. To determine the anatomical locations of compromised mechanical performance bone, nanoindentation tests (corrected for amount of mineral present based on qBEI analysis) were performed. The results indicated that the mechanical performance differences between control and β-APN treated animals are limited to areas of lower mineralization, a logical outcome given the fact that the β-APN effect on bone was necessarily restricted to bone that was formed during the period of treatment. It is also in the same anatomical areas that the spectroscopically determined collagen cross-link ratio (Pyd/divalent) was altered. The fact that there were no differences in these bone areas between the animals either in mineral content or in maturity/crystallinity suggests that the observed differences in mechanical properties were due to alterations of collagen. In this context it may be worth remarking that small local confined changes in mechanical properties of a composite material are not likely to affect the overall modulus of the bone material, which is always an average (though not necessarily an arithmetic average) of the local properties. However, it may have a profound effect on its strength, because strength depends essentially on the strength of the weakest link in the chain. This seems to fit well also to the observation in the present study that the overall modulus of whole bone is essentially not affected, while the strength is reduced.

It should be kept in mind when considering the results of the present study that not all of the expected changes in collagen due to β-APN administration were monitored. For example, we did not analyze for pyrroles (important trivalent cross-links), as no microspectroscopic parameters have been developed to date describing them, thus the anatomical spatial distribution could not be established.

In summary, the results of the present study show the good correspondence between biochemically and spectroscopically determined pyd/divalent collagen cross-link ratio. They suggest that normalization for tissue age is critical as it excludes interference in the results from specimen age induced variability. They also indicate that collagen cross-link alterations, even when limited to certain anatomical areas (as in the case of the present study where they were confined to bone forming areas only), coupled with structural properties alterations are capable of affecting the mechanical performance of the whole bone. Moreover, they are capable of doing so even in the absence of concomitant alterations in mineral content (as determined by qBEI) and quality (as determined by FTIR). This may be of particular importance since previously published analysis of human iliac crest biopsies from osteoporotic and non-osteoporotic (based on the classical clinical criteria) patients sustaining atraumatic or low trauma fragility fractures shows similar results as far as collagen cross-link ratio is concerned [17,18]. Additionally, the results were obtained in vertebrae, and the incidence of vertebral fractures in osteoporosis is twice that of hip fractures [70], although caution should be exercised as an animal model was employed in the present study. These results become even more important in view of the recent clinical reports, which have correlated plasma homocysteine levels and bone fragility [12–15] when it is noted that the mechanism by which homocysteine and β-APN block collagen cross-link formation is analogous.

Conflict of interest

None of the authors have any conflict of interest.

Acknowledgments

The authors thank Gerda Dinst, Sabrina Thon, Phaedra Messmer, and Daniela Gabriel for careful sample preparations and qBEI measurements at the Bone Material Laboratory of the Ludwig Boltzmann-Institute of Osteology, Vienna, Austria. This study was supported by the Allgemeine Unfallversicherungsanstalt (AUVA), research funds of the Austrian workers compensation board; the Wiener Gebietskrankenkasse (WGKK), Viennese sickness insurance funds; and the Fonds zur Foederung der wissenschaftlichen Forschung (FWF); the Division of Periodontology, Ohio State University; a research grant from the Alliance for Better Bone Health (to EPP); NIH grant AR046505 (to EPP).

References

[1] Albright F, Reifenstein EC. The parathyroid glands and metabolic bone disease. Baltimore, MD: Williams and Wilkins; 1948.
[2] Fratzl P, Gupta H, Paschalis E, Roschger P. Structure and mechanical quality of the collagen–mineral nano-composite in bone. J Mater Chem 2004;14:2115–23.
[3] Yamauchi M. Collagen: the major matrix molecule in mineralized tissues. In: Anderson JJB, Garner SC, editors. Calcium and phosphorus in health and disease. New York: CRC Press; 1996. p. 127–41.
[4] Hansen DA, Eyre DR. Molecular site specificity of pyridinoline and pyrrole cross-links in type I collagen of human bone. J Biol Chem 1996;271:26508–16.
[5] Kuypers R, Tyler M, Kurth LB, Jenkins ID, Hogan DJ. Identification of the loci of the collagen-associated Ehrlich chromogen in type I collagen confirms its role as a trivalent cross-link. Biochem J 1992;283:129–36.
[6] Knott L, Tarlton JF, Bailey AJ. Chemistry of collagen cross-linking: biochemical changes in collagen during the partial mineralization of turkey leg tendon. Biochem J 1997;322:535–42.
[7] Brady JD, Robins SP. Structural characterization of pyrrolic cross-links in collagen using a biotinylated Ehrlich's reagent. J Biol Chem 2001;276:18812–8.

[8] Robins SP. Biochemistry and functional significance of collagen cross-linking. Biochem Soc Trans 2007;35:849–52.
[9] Nyman JS, Roy A, Acuna RL, Gayle HJ, Reyes MJ, Tyler JH, et al. Age-related effect on the concentration of collagen crosslinks in human osteonal and interstitial bone tissue. Bone 2006;39:1210–7.
[10] Saito M, Marumo K. Collagen cross-links as a determinant of bone quality: a possible explanation for bone fragility in aging, osteoporosis, and diabetes mellitus. Osteoporos Int 2010;21:195–214.
[11] Tang SY, Zeenath U, Vashishth D. Effects of non-enzymatic glycation on cancellous bone fragility. Bone 2007;40:1144–51.
[12] Gjesdal CG, Vollset SE, Ueland PM, Refsum H, Meyer HE, Tell GS. Plasma homocysteine, folate, and vitamin B 12 and the risk of hip fracture: the hordaland homocysteine study. J Bone Miner Res 2007;22:747–56.
[13] McLean RR, Hannan MT. B vitamins, homocysteine, and bone disease: epidemiology and pathophysiology. Curr Osteoporos Rep 2007;5:112–9.
[14] McLean RR, Jacques PF, Selhub J, Fredman L, Tucker KL, Samelson EJ, et al. Plasma B vitamins, homocysteine, and their relation with bone loss and hip fracture in elderly men and women. J Clin Endocrinol Metab 2008;93:2206–12.
[15] McLean RR, Jacques PF, Selhub J, Tucker KL, Samelson EJ, Broe KE, et al. Homocysteine as a predictive factor for hip fracture in older persons. N Engl J Med 2004;350:2042–9.
[16] Blouin S, Thaler HW, Korninger C, Schmid R, Hofstaetter JG, Zoehrer R, et al. Bone matrix quality and plasma homocysteine levels. Bone 2009;44:959–64.
[17] Paschalis EP, Recker R, DiCarlo E, Doty SB, Atti E, Boskey AL. Distribution of collagen cross-links in normal human trabecular bone. J Bone Miner Res 2003;18:1942–6.
[18] Paschalis EP, Shane E, Lyritis G, Skarantavos G, Mendelsohn R, Boskey AL. Bone fragility and collagen cross-links. J Bone Miner Res 2004;19:2000–4.
[19] Gourion-Arsiquaud S, Faibish D, Myers E, Spevak L, Compston J, Hodsman A, et al. Use of FTIR spectroscopic imaging to identify parameters associated with fragility fracture. J Bone Miner Res 2009;24:1565–71.
[20] Blank RD, Baldini TH, Kaufman M, Bailey S, Gupta R, Yershov Y, et al. Spectroscopically determined collagen Pyr/deH-DHLNL cross-link ratio and crystallinity indices differ markedly in recombinant congenic mice with divergent calculated bone tissue strength. Connect Tissue Res 2003;44:134–42.
[21] Paschalis EP, Glass EV, Donley DW, Eriksen EF. Bone mineral and collagen quality in iliac crest biopsies of patients given teriparatide: new results from the fracture prevention trial. J Clin Endocrinol Metab 2005;90:4644–9.
[22] Oxlund H, Barckman M, Ortoft G, Andreassen TT. Reduced concentrations of collagen cross-links are associated with reduced strength of bone. Bone 1995;17:365S–71S.
[23] Spengler DM, Baylink DJ, Rosenquist JB. Effect of beta-aminopropionitrile on bone mechanical properties. J Bone Joint Surg Am 1977;59:670–2.
[24] Wegedal JE. Enzymes of protein and phosphate catabolism in rat bone. I. Enzyme properties in normal rats. Calcif Tissue Res 1969;3:55–66.
[25] Robins SP, Milne G, Duncan A, Davies C, Butt R, Greiling D, et al. Increased skin collagen extractability and proportions of collagen type III are not normalized after 6 months healing of human excisional wounds. J Invest Dermatol 2003;121:267–72.
[26] Roschger P, Paschalis EP, Fratzl P, Klaushofer K. Bone mineralization density distribution in health and disease. Bone 2008;42:456–66.
[27] Fratzl-Zelman N, Roschger P, Gourrier A, Weber M, Misof BM, Loveridge N, et al. Combination of nanoindentation and quantitative backscattered electron imaging revealed altered bone material properties associated with femoral neck fragility. Calcif Tissue Int 2009;85:335–43.
[28] Manjubala I, Liu Y, Epari DR, Roschger P, Schell H, Fratzl P, et al. Spatial and temporal variations of mechanical properties and mineral content of the external callus during bone healing. Bone 2009;45:185–92.
[29] Oliver W, Pharr G. An improved technique for determining hardness and elastic-modulus using load and displacement sensing indentation experiments. J Mater Res 1992;7:1564–83.
[30] Boskey AL, Pleshko N, Doty SB, Mendelsohn R. Applications of Fourier transform infrared (FT-IR) microscopy to the study of mineralization in bone and cartilage. Cells Mater 1992;2:209–20.
[31] Gadaleta SJ, Paschalis EP, Betts F, Mendelsohn R, Boskey AL. Fourier transform infrared spectroscopy of the solution-mediated conversion of amorphous calcium phosphate to hydroxyapatite: new correlations between X-ray diffraction and infrared data. Calcif Tissue Int 1996;58:9–16.
[32] Paschalis EP, DiCarlo E, Betts F, Sherman P, Mendelsohn R, Boskey AL. FTIR microspectroscopic analysis of human osteonal bone. Calcif Tissue Int 1996;59:480–7.
[33] Paschalis EP, Verdelis K, Doty SB, Boskey AL, Mendelsohn R, Yamauchi M. Spectroscopic characterization of collagen cross-links in bone. J Bone Miner Res 2001;16:1821–8.
[34] Bailey AJ, Wotton SF, Sims TJ, Thompson PW. Biochemical changes in the collagen of human osteoporotic bone matrix. Connect Tissue Res 1993;29:119–32.
[35] Banse X. When density fails to predict bone strength. Acta Orthop Scand Suppl 2002;73:1–57.
[36] Banse X, Sims TJ, Bailey AJ. Mechanical properties of adult vertebral cancellous bone: correlation with collagen intermolecular cross-links. J Bone Miner Res 2002;17:1621–8.
[37] Knott L, Whitehead CC, Fleming RH, Bailey AJ. Biochemical changes in the collagenous matrix of osteoporotic avian bone. Biochem J 1995;310:1045–51.
[38] Kowitz J, Knippel M, Schuhr T, Mach J. Alteration in the extent of collagen I hydroxylation, isolated from femoral heads of women with a femoral neck fracture caused by osteoporosis. Calcif Tissue Int 1997;60:501–5.
[39] Oxlund H, Mosekilde L, Ortoff G. Alterations in the stability of collagen from human trabecular bone with respect to age. In: Christiansen C, Johansen JS, Riis BJ, editors. Osteoporosis 1987. Copenhagen: Osteopress APS; 1987. p. 309–12.
[40] Banse X, Devogelaer JP, Lafosse A, Sims TJ, Grynpas M, Bailey AJ. Cross-link profile of bone collagen correlates with structural organization of trabeculae. Bone 2002;31:70–6.
[41] Smith LJ, Schirer JP, Fazzalari NL. The role of mineral content in determining the micromechanical properties of discrete trabecular bone remodeling packets. J Biomech 2010;43:3144–9.
[42] Zebaze RM, Jones AC, Pandy MG, Knackstedt MA, Seeman E. Differences in the degree of bone tissue mineralization account for little of the differences in tissue elastic properties. Bone 2011;48(6):1246–51.
[43] Gao H, Ji B, Jager IL, Arzt E, Fratzl P. Materials become insensitive to flaws at nanoscale: lessons from nature. Proc Natl Acad Sci USA 2003;100:5597–600.
[44] Jager I, Fratzl P. Mineralized collagen fibrils: a mechanical model with a staggered arrangement of mineral particles. Biophys J 2000;79:1737–46.
[45] Bailey AJ, Knott L. Molecular changes in bone collagen in osteoporosis and osteoarthritis in the elderly. Exp Gerontol 1999;34:337–51.
[46] Bailey AJ, Wotton SF, Sims TJ, Thompson PW. Post-translational modifications in the collagen of human osteoporotic femoral head. Biochem Biophys Res Commun 1992;185:801–5.
[47] Knott L, Bailey AJ. Collagen cross-links in mineralizing tissues: a review of their chemistry, function, and clinical relevance. Bone 1998;22:181–7.
[48] Masse PG, Boskey AL, Pritzker KPH, Mendes M, Weiser H. Vitamin B_6 deficiency experimentally-induced bone and joint disorder: microscopic, radiographic and biochemical evidence. Br J Nutr 1994;71:919–32.
[49] Masse PG, Colombo VE, Gerber F, Howell DS, Weiser H. Morphological abnormalities in vitamin B_6 deficient tarsometatarsal chick cartilage. Scanning Microsc 1990;4:667–74.
[50] Masse PG, Rimnac CM, Yamauchi M, Coburn PS, Rucker BR, Howell SD, et al. Pyridoxine deficiency affects biomechanical properties of chick tibial bone. Bone 1996;18:567–74.
[51] Prockop DJ, Kivirikko KI. Heritable diseases of collagen. N Engl J Med 1984;311:376–96.
[52] Golub L, Stern B, Glimcher M, Goldhaber P. The inhibition of the maturation of newly synthesized bone collagen by beta-aminopropionitrile in tissue culture. Proc Soc Exp Biol Med 1968;129:465–9.
[53] Golub L, Stern B, Glimcher M, Goldhaber P. The effect of a lathyrogenic agent on the synthesis and degradation of mouse bone collagen in tissue culture. Arch Oral Biol 1968;13:1395–8.
[54] Golub L, Stern B, Glimcher M, Goldhaber P. The effect of lathyrism on bone collagen metabolism in tissue culture. J Periodontol 1968;39:44–5.
[55] Henneman DH. Inhibition by estradiol-17 beta of the lathyritic effect of beta-aminopropionitrile (BAPN) on skin and bone collagen. Clin Orthop Relat Res 1972;83:245–54.
[56] Shimizu M, Golub L, Glimcher M. The effect of lathyrogens on the rate of collagen fibril formation and dissolution. Biochim Biophys Acta 1968;168:356–8.
[57] Paschalis EP, Mendelsohn R, Boskey AL. Infrared assessment of bone quality: a review. Clin Orthop Relat Res 2011;469(8):2170–8.
[58] Bloebaum R, Skedros J, Vajda E, Bachus K, Constantz P. Determining mineral content variations in bone using backscattered electron imaging. Bone 1997;20:485–90.
[59] Donnelly E, Chen DX, Boskey AL, Baker SP, van der Meulen MC. Contribution of mineral to bone structural behavior and tissue mechanical properties. Calcif Tissue Int 2010;87:450–60.
[60] Camacho NP, Rimnac CM, Meyer Jr RA, Doty S, Boskey AL. Effect of abnormal mineralization on the mechanical behavior of X-linked hypophosphatemic mice femora. Bone 1995;17:271–8.
[61] Courtland HW, Nasser P, Goldstone AB, Spevak L, Boskey AL, Jepsen KJ. Fourier transform infrared imaging microspectroscopy and tissue-level mechanical testing reveal intraspecies variation in mouse bone mineral and matrix composition. Calcif Tissue Int 2008;83:342–53.
[62] Thaler R, Spitzer S, Rumpler M, Fratzl-Zelman N, Klaushofer K, Paschalis EP, et al. Differential effects of homocysteine and beta aminopropionitrile on preosteoblastic MC3T3-E1 cells. Bone 2010;46:703–9.
[63] Turecek C, Fratzl-Zelman N, Rumpler M, Buchinger B, Spitzer S, Zoehrer R, et al. Collagen cross-linking influences osteoblastic differentiation. Calcif Tissue Int 2008;82:392–400.
[64] Chevalier Y, Pahr D, Zysset PK. The role of cortical shell and trabecular fabric in finite element analysis of the human vertebral body. J Biomech Eng 2009;131:111003.
[65] Christiansen BA, Kopperdahl DL, Kiel DP, Keaveny TM, Bouxsein ML. Mechanical contributions of the cortical and trabecular compartments contribute to differences in age-related changes in vertebral body strength in men and women assessed by QCT-based finite element analysis. J Bone Miner Res 2011;26:974–83.
[66] Melton III LJ, Riggs BL, Keaveny TM, Achenbach SJ, Kopperdahl D, Camp JJ, et al. Relation of vertebral deformities to bone density, structure, and strength. J Bone Miner Res 2010;25:1922–30.
[67] Szulc P, Boutroy S, Vilayphiou N, Chaitou A, Delmas PD, Chapurlat R. Cross-sectional analysis of the association between fragility fractures and bone microarchitecture in older men: the STRAMBO study. J Bone Miner Res 2011;26:1358–67.
[68] Vilayphiou N, Boutroy S, Szulc P, van Rietbergen B, Munoz F, Delmas PD, et al. Finite element analysis performed on radius and tibia HR-pQCT images and fragility fractures at all sites in men. J Bone Miner Res 2011;26:965–73.
[69] Wegrzyn J, Roux JP, Arlot ME, Boutroy S, Vilayphiou N, Guyen O, et al. Determinants of the mechanical behavior of human lumbar vertebrae after simulated mild fracture. J Bone Miner Res 2011;26:739–46.
[70] Cooper C, Melton L. Magnitude and impact of osteoporosis and fractures. In: Marcus R, Feldman D, Kelsey J, editors. Osteoporosis. London: Academic press Inc.; 1996. p. 425.